

Feynman Diagrams and Cutting Rules

J.S. Rozowsky¹

Department of Physics, University of California at Los Angeles, CA 90095-1547

Abstract

We show how Feynman diagrams may be evaluated to take advantage of recent developments in the application of Cutkosky rules to the calculation of one-loop amplitudes. A sample calculation of $gg \rightarrow gH$, previously calculated by Ellis et al., is presented illustrating this equivalence. This example demonstrates the use of cutting rules for massive amplitudes.

¹Email address: rozowsky@physics.ucla.edu

1 Introduction

One-loop calculations are important in the quest for discovering new physics beyond the Standard Model, especially for determining QCD backgrounds. A number of significant improvements in the calculation of one-loop amplitudes, especially ones with massless particles, have been made in recent years. These methods, which have recently been reviewed in ref. [1], include the use of helicity [2], color decompositions [3], string-inspired ideas [4], recursion relations [5, 6], unitarity [7, 8, 9, 10] and factorization [11]. Besides allowing for the computation of certain infinite sequences of amplitudes, these techniques have been used in the computation of non-trivial amplitudes relevant for phenomenological applications [12, 13].

A technique that has proven to be especially useful is that of using unitarity to determine the functional form of the amplitudes. By working to all orders in the dimensional regularization parameter, $\epsilon = (4 - D)/2$, one can determine the coefficients of all integral functions that may appear [14]. For certain amplitudes that satisfy a power counting criterion, such as supersymmetric ones, one can show that cuts with four-dimensional momenta are sufficient to determine the amplitudes through $\mathcal{O}(\epsilon^0)$ [8, 9]. The case of an amplitude with massive internal legs has been considered in ref. [10].

The efficiency of the unitarity method stems from the use of gauge invariant tree amplitudes in performing calculations. With the use of helicity and color decompositions this can lead to enormous reductions in the complexity of intermediate expressions. This may be contrasted against calculations of individual Feynman diagrams that are gauge variant, where large cancelations must take place in order to obtain simpler gauge invariant results.

In this paper we will show how to evaluate Feynman diagrams so as to obtain efficiency of computation inherent in the unitarity technique. This is done by performing Feynman diagram calculations in a particular way so as to mimic the unitarity approach advocated in ref. [1]. One may therefore start with Feynman diagrams, yet obtain the advantages of the Cutkosky approach. This is useful since it explains the unitarity method from a conventional Feynman diagram viewpoint. This is of interest in, for example, the extension of unitarity methods beyond one loop, such as in ref. [15].

As an explicit example we have calculated the one-loop helicity amplitudes for $gg \rightarrow gH$. This example has the desirable features that it contains both colored and colorless lines and massive internal and external legs. This example is useful since it illustrates features beyond purely massless calculations, where most attention has been concentrated [1]. Also it has already been evaluated via conventional methods by R.K. Ellis et al. [16], allowing for an easy comparison to the correct result to be made. We find agreement with their result.

2 Review of basic tools

We now briefly review some of the techniques that we shall use in this paper. Two important techniques that we utilize are spinor helicity and color decomposition. The reader may consult review articles [17] for further details.

2.1 Spinor helicity

In explicit calculations with external gluons, it is usually convenient to use a spinor helicity basis [2] which rewrites all polarization vectors in terms of massless Weyl spinors $|k^\pm\rangle$. In the formulation of Xu, Zhang and Chang the plus and minus helicity polarization vectors are expressed as

$$\varepsilon_\mu^+(k; q) = \frac{\langle q^- | \gamma_\mu | k^- \rangle}{\sqrt{2} \langle q k \rangle}, \quad \varepsilon_\mu^-(k; q) = \frac{\langle q^+ | \gamma_\mu | k^+ \rangle}{\sqrt{2} [k q]}, \quad (2.1)$$

where k is the momentum of the gluon and q is an arbitrary null ‘reference momentum’ which drops out of the final gauge invariant amplitudes. We use the convenient notation

$$\langle k_i^- | k_j^+ \rangle \equiv \langle ij \rangle, \quad \langle k_i^+ | k_j^- \rangle \equiv [ij]. \quad (2.2)$$

These spinor products are anti-symmetric and satisfy $\langle ij \rangle [ji] = 2k_i \cdot k_j$. One useful identity is

$$\langle a | \not{\epsilon}^\pm(k; q) | b \rangle = \pm \frac{\sqrt{2}}{\langle q^\mp | k^\pm \rangle} \langle a | [|q^\pm\rangle \langle k^\pm| + |k^\mp\rangle \langle q^\mp|] | b \rangle, \quad (2.3)$$

where either $\langle a |$ or $| b \rangle$ are spinors with four-dimensional momenta.

It is convenient to choose a dimensional regularization scheme that is compatible with the spinor helicity formalism. We use the four-dimensional helicity scheme [4] which is equivalent to a helicity form of Siegel’s dimensional reduction scheme [18]. The conversion between the various dimensional regularization schemes has been given in ref. [4, 19].

2.2 Color decomposition

Color decompositions [3] have been extensively discussed in review articles [17]. Here we only present the color decomposition for the $gg \rightarrow gH$ amplitude.

For this one-loop amplitude the decomposition is

$$\mathcal{A}_4^{1\text{-loop}} = g^3 \mu_R^{2\epsilon} \sum_\sigma \text{tr}[T^{a_{\sigma(1)}} T^{a_{\sigma(2)}} T^{a_{\sigma(3)}}] A_4^f(\sigma(1), \sigma(2), \sigma(3), H), \quad (2.4)$$

where we have taken the loop to be in the fundamental representation. The sum over σ includes all cyclic permutations of the indices $\sigma(n)$ (i.e. $\sigma \in \{(1, 2, 3), (1, 3, 2)\}$) and the T^a are fundamental representation color matrices (normalized so that $\text{tr}(T^a T^b) = \delta^{ab}$). We have abbreviated the dependence of A_4^f on the outgoing momenta k_j and helicities λ_j by writing the label j alone. We have also explicitly extracted the coupling and a factor of $\mu_R^{2\epsilon}$ from A_4^f , where μ_R is the renormalization scale. For adjoint representation loops there is an analogous decomposition with up to two color traces in each term.

It is convenient to further decompose the partial amplitude in terms of *primitive amplitudes*,

$$\begin{aligned} & A_4^f(\sigma(1), \sigma(2), \sigma(3), H) \\ &= A_4(\sigma(1), \sigma(2), \sigma(3), H) + A_4(\sigma(3), \sigma(1), \sigma(2), H) + A_4(\sigma(2), \sigma(3), \sigma(1), H). \end{aligned} \quad (2.5)$$

In the primitive amplitudes appearing on the right-hand-side we may treat the Higgs as carrying color charge (in the adjoint representation), which couples to gluons; it is not difficult to show in the permutation sum all such additional terms cancel. This is convenient since these primitive amplitudes are gauge invariant and have a fixed cyclic ordering of external legs. A similar decomposition in terms of ‘primitive amplitudes’ can also be performed for the case where some of the external particles are in the fundamental representation [20].

3 Feynman diagrams

Feynman diagrams, which have been essential for evaluating terms in the perturbative series for scattering processes, suffer from a number of well known computational difficulties. Firstly, individual Feynman diagrams are inherently gauge dependent; gauge invariance is restored only after summing over all diagrams. Secondly, when evaluating loop momentum integrals using traditional techniques, such as Passarino-Veltman reduction [21], one encounters a large number of spurious denominators. These spurious denominators typically involve Gram determinants, $\det(k_i \cdot k_j)$ raised to a power. Enormous cancelations must then take place before one obtains relatively simple results.

When using conventional techniques to evaluate Feynman diagrams one reduces all tensor integrals into sums of scalar integrals multiplied by reduction coefficients. (By a tensor integral we mean loop momentum integrals with powers of momentum in the numerator and by a scalar integral we mean integrals with no powers of loop momentum in the numerator, see appendix A.) With the knowledge of how this reduction works, given any one-loop amplitude we can list all the scalar integrals that could potentially enter. Thus we have

$$\text{Amplitude} = \sum \text{Feynman diagrams} \rightarrow \sum_i c_i I_i, \quad (3.1)$$

where the subscript i is some index that labels the scalar integrals that contribute to this amplitude. The heart of the calculation is in evaluating all the coefficients of the scalar integrals, i.e. the c_i 's.

A conventional Feynman diagram technique like Passarino-Veltman (PV) reduction evaluates all the necessary coefficients simultaneously. If one could obtain these coefficients in a more efficient manner one would greatly improve the ability to calculate.

Some of the features that are useful in improved calculational methods are: (1) that the building blocks be gauge invariant combinations of diagrams instead of individual diagrams; (2) that wherever possible tensor integrals should not generate large powers of Gram determinants in denominators; (3) that large cancelations between diagrams be avoided as much as possible; (4) and that calculations can be recycled when performing new ones.

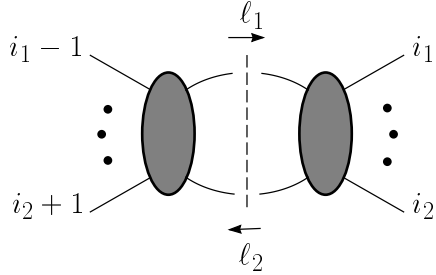


Figure 1: A cut of a general n -point one-loop amplitude.

3.1 Review of the unitarity method

The cutting method reviewed in ref. [1] has these above properties. In this method one writes down the cuts in a given channel, depicted in fig. 1,

$$A_n(1, 2, \dots, n) \Big|_{\text{cut}} = \int \frac{d^{4-2\epsilon} p}{(2\pi)^{4-2\epsilon}} \frac{i}{\ell_1^2 - m_1^2} A_{n_1}^{\text{tree}}(-\ell_1, i_1, \dots, i_2, \ell_2) \frac{i}{\ell_2^2 - m_2^2} A_{n_2}^{\text{tree}}(-\ell_2, i_2 + 1, \dots, i_1 - 1, \ell_1) \Big|_{\text{cut}}. \quad (3.2)$$

This equation is valid only for the cut channel under consideration. The loop momentum is p ; ℓ_1 and ℓ_2 are the momenta of the cut propagators, with masses m_1 and m_2 respectively and $n_1 + n_2 = n + 4$. One then reconstructs the complete amplitude by finding a function which has the correct cuts in *all* channels.

Since the loop integral in eq. (3.2) is composed of products of on-shell tree amplitudes, the basic building blocks are gauge invariant. These tree amplitudes are inherently easier to calculate than loop amplitudes and in many cases have been previously calculated. A key feature of the cutting method is that a specific subset of scalar integral coefficients are obtained in any given channel. Then one repeats this process for various channels thus computing the coefficients for all the scalar integrals. There are integrals that do not appear in any channel, namely the tadpole and scalar bubble integrals,

$$I_1^{D=4-2\epsilon} \quad \text{and} \quad \lim_{k^2 \rightarrow 0} I_2^{D=4-2\epsilon}(k^2). \quad (3.3)$$

However, with prior knowledge of the infrared and ultraviolet behavior of an amplitude in many cases the coefficients of these integrals can be fixed, as discussed in ref. [10].

It is generally convenient to express the tree amplitudes in eq. (3.2) using the spinor helicity formalism discussed in section 2.1. Then one can evaluate the right-hand side of eq. (3.2) by constructing spinor strings of the form $\langle a | \dots \ell_1 \dots \ell_2 \dots | b \rangle$, and then commuting the ℓ_i towards each other. This generates terms of the form $\ell_i \cdot k_j$, which may be rewritten as differences of inverse propagators and terms which do not depend on the loop momentum. This type of reduction procedure has been previously used in a number of references [8, 9, 10, 22]. We shall make use of it in the next section.

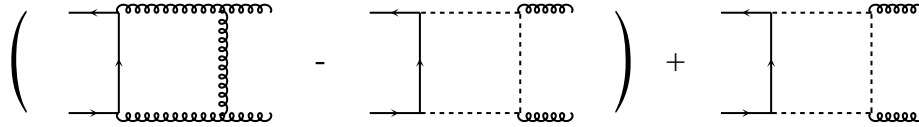


Figure 2: The contribution from a vector in the loop is separated into the difference of a vector and scalar plus a scalar so that the difference satisfies the power-counting criterion.

When using spinor helicity one must take into account that the momenta of the intermediate on-shell lines are in $(4 - 2\epsilon)$ dimensions while the helicity formalism is defined in four dimensions. If one drops the (-2ϵ) -dimensional components of the momenta, one could make an error in rational functions arising from ϵ/ϵ terms. For five- and higher-point calculations it can be more convenient to use four-dimensional momenta in the cuts, but then to reconstruct the missing rational functions using collinear and multi-particle factorization properties [11, 1]. For four-point calculations it is convenient to keep terms to all orders in ϵ , since factorization is insufficient to fix all rational functions.

The cases of fermion or scalar lines with $(4 - 2\epsilon)$ momenta in the helicity formalism have been extensively discussed in ref. [10] and do not present any difficulties. Although it is unnecessary for the specific calculation $gg \rightarrow gH$, a convenient strategy for handling channels with gluon lines is to subtract and add equivalent diagrams with internal gluon lines replaced by scalar or fermion lines, as depicted in fig. 2. In some cases one uses fermions so as to group particles together with supersymmetric partners. Such combinations of diagrams satisfy the power counting criterion that n -point tensor integrals should have (for $n > 2$) at most $n - 2$ powers of loop momentum in the numerator of the integrand; two-point integrals should have at most one power of loop momentum. The required rearrangement of the diagrams to make the power count apparent is discussed in ref. [9]. In particular, for the example portrayed in fig. 2 one should use background field Feynman gauge [23]. The origin of this power counting criterion is from the requirement that all contributions due to the $\mathcal{O}(\epsilon)$ parts of loop momenta should not interfere with ultraviolet poles to yield $\mathcal{O}(\epsilon^0)$ contributions. (One can also show that infrared divergences never interfere with the $\mathcal{O}(\epsilon)$ parts of loop momenta [9].) This criterion also holds for the general massive amplitudes discussed in this paper. This is useful since one can then take the sewed gluon lines to have four-dimensional momenta without any errors through $\mathcal{O}(\epsilon^0)$.

3.2 From Feynman diagrams to the unitarity method

We now describe how to perform a Feynman diagram calculation so as to mimic the cutting method. In the next section we give an explicit example involving both internal and external masses. The basic idea is rather simple.

Given that we know all the scalar integrals that could possibly enter a one-loop amplitude,

suppose we target those scalar integrals that have a pair of scalar propagators

$$i/(\ell_1^2 - m_1^2) \quad \text{and} \quad i/(\ell_2^2 - m_2^2), \quad (3.4)$$

where ℓ_1 is the momentum of the scalar propagator between external legs $i_1 - 1$ and i_1 , and ℓ_2 is between i_2 and $i_2 + 1$ of a general n -point amplitude, where the indicated propagators are each of a specific particle type. In order to generate a scalar integral with a specific propagator one must necessarily have evaluated a Feynman diagram that has the corresponding propagator.

We can define a channel (this channel will correspond to the cut-channel when the cut is performed on the indicated legs) as a subset of the terms in the full amplitude; the terms being the scalar integrals which include the pair of scalar propagators mentioned above together with their corresponding coefficients, the c_i 's.

In each Feynman integral (the tensor integral corresponding to each Feynman diagram) we explicitly extract a denominator that includes the pair of scalar propagators under consideration. Then if we impose the on-shell conditions $\ell_1^2 - m_1^2 = \ell_2^2 - m_2^2 = 0$ to the numerators of all the Feynman integrals contributing to the amplitude then the result would yield exactly what we defined as a channel in the previous paragraph. The potential errors when imposing these on-shell conditions would necessarily be of the form

$$\int \frac{d^D \ell}{(2\pi)^D} \frac{(\ell_1^2 - m_1^2)^n (\ell_2^2 - m_2^2)^m f(\ell_1, \ell_2, \dots)}{\dots (\ell_1^2 - m_1^2) (\ell_2^2 - m_2^2) \dots}, \quad (3.5)$$

where $n \geq 1$ and/or $m \geq 1$, and $D = 4 - 2\epsilon$. Since $(\ell_1^2 - m_1^2)$ and $(\ell_2^2 - m_2^2)$ are themselves inverse scalar propagators, anything of the form of eq. (3.5) could only generate terms which are not in the channel under consideration. This is because one or both of the inverse propagators would cancel a scalar propagator in the denominator and generate a scalar integral not included in the specified channel, i.e. that does not include both of the indicated scalar propagators. Setting $\ell_1^2 - m_1^2 = \ell_2^2 - m_2^2 = 0$ only affects the calculation of those terms not in the specified channel. Thus the evaluation of the c_i 's that are in the specified channel are not affected by imposing the on-shell condition.

By systematically stepping through a sufficient number of channels one can fix all the coefficients, the c_i 's in eq. (3.1). In this way we can reconstruct the full amplitude. For some coefficients the corresponding integrals appear in multiple channels; for consistency these must coincide.

So how does using the on-shell conditions $\ell_1^2 - m_1^2 = \ell_2^2 - m_2^2 = 0$ in the numerator help us in evaluating the Feynman diagrams? All Feynman diagrams in a specific channel can now be 'factorized' using their on-shell legs into the sewing of two Feynman tree diagrams (see fig. 3).

In figure fig. 3 the 'factorized' Feynman graph only contains intermediate on-shell fermions for the $gg \rightarrow gH$ amplitude. But in general this 'factorization' process can be performed on any one-loop Feynman diagram. With on-shell scalars or fermions it is clear that this can be done. With intermediate massless gauge particles one might worry that one has forgotten about the contributions of diagrams with ghosts on the right hand side of fig. 3.

$$\begin{array}{c}
\text{H} \text{---} \ell_1 \\
\uparrow \quad \downarrow \\
3 \text{---} \ell_2 \text{---} 1 \\
\downarrow \quad \uparrow \\
\ell_2 \text{---} 2
\end{array}
= \sum_{\text{helicity}} \int \frac{d^D \ell}{(2\pi)^D}
\begin{array}{c}
\text{H} \text{---} \ell_1 \\
\uparrow \\
3 \text{---} \ell_2
\end{array}
\times \frac{i}{(\ell_1^2 - m_1^2)} \frac{i}{(\ell_2^2 - m_2^2)} \times
\begin{array}{c}
\ell_1 \text{---} 1 \\
\downarrow \\
\ell_2 \text{---} 2
\end{array}
\Big|_{\ell_1^2 - m_1^2 = \ell_2^2 - m_2^2 = 0}$$

Figure 3: An example of a Feynman graph for the $gg \rightarrow gH$ amplitude that contributes to the s -channel, ‘factorized’ into the sewing of two trees. The dashed lines on the left hand side indicate the on-shell propagators and the helicity sum is over the polarizations of the ‘factorized’ legs.

We know, however, that the net effect of the one-loop diagrams with ghosts is to cancel the unphysical polarizations of graphs with corresponding gauge particles. This cancelation can be made apparent using the background field Feynman gauge [23]. However, once one has ‘factorized’ a Feynman graph on a pair of propagators that includes a gauge particle then the contribution of the ghosts is not necessary as the sewing of the two on-shell Feynman trees manifestly has no unphysical gauge degrees of freedom.

If one sums over all the Feynman diagrams that contribute to a specific channel and we impose the on-shell condition then the equivalent equation to fig. 3 would have on-shell tree amplitudes sewed together instead of on-shell Feynman trees:

$$\begin{aligned}
A_n(1, 2, \dots, n)|_{\text{channel}} = \sum_{\text{helicity}} \int \frac{d^{4-2\epsilon} \ell}{(2\pi)^{4-2\epsilon}} A_{n_1}^{\text{tree}}(-\ell_1, i_1, \dots, i_2, \ell_2) \frac{i}{(\ell_1^2 - m_1^2)} \frac{i}{(\ell_2^2 - m_2^2)} \\
\times A_{n_2}^{\text{tree}}(-\ell_2, i_2 + 1, \dots, i_1 - 1, \ell_1) \Big|_{\ell_1^2 - m_1^2 = \ell_2^2 - m_2^2 = 0}.
\end{aligned} \tag{3.6}$$

The sum on the right-hand side runs over all helicity states that can propagate across the ‘cut’ legs. Using the above equation one can compute all the coefficients of the scalar integrals that appear in this channel.

The above equation, eq. (3.6), is the unitarity method mentioned earlier in this section. Originally the method was inspired by Cutkosky rules, however, from the arguments presented here it is clear that one can evaluate Feynman diagrams in a sophisticated manner so as to take advantage of the benefits inherent in the unitarity method. Instead of performing the calculation of the scalar integral coefficients in parallel, we perform the calculation by targeting simultaneously only those integrals in a given channel.

The notion of channels presented in this section is more general than that of just considering Cutkosky rules because we may use the on-shell conditions on any propagator which does not collapse in the integral function under consideration. (Indeed, this observation has already been used in calculations of $Z \rightarrow 4$ partons [13].) In general we could construct a channel where we use the on-shell condition for any number of propagators (it is even possible to construct a channel where the on-shell condition is used for a single propagator); however, it is normally convenient to use only the two-propagator channel construction.

4 Calculation of $gg \rightarrow gH$

In this section we apply the procedure outlined in the previous section to the specific example of $gg \rightarrow gH$. This amplitude has one massive external leg and all the Feynman diagrams have a massive quark running in the loop. See fig. 4 for the color-ordered Feynman diagrams contributing to this amplitude.

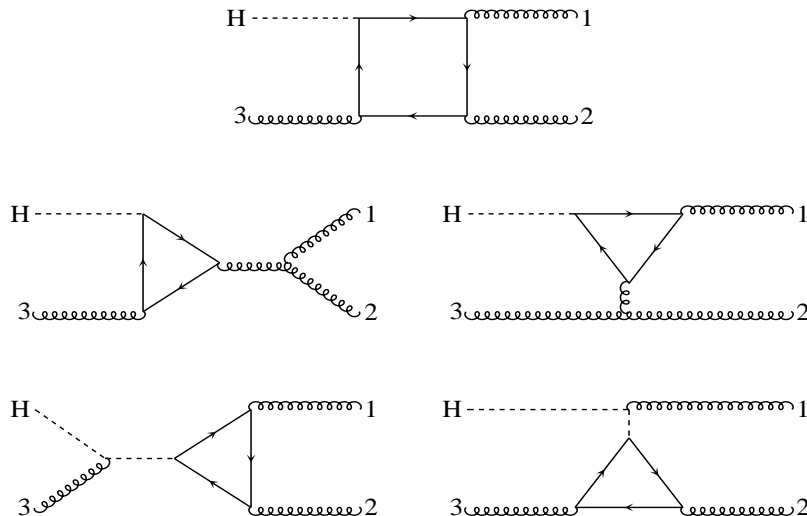


Figure 4: The color-ordered Feynman diagrams contributing to the amplitude $gg \rightarrow gH$.

In fig. 4 there are two Feynman diagrams that involve a Higgs-Higgs-gluon coupling which does not exist in the Standard Model. As mentioned in section 2.2, although these diagrams cancel from the final result, they make the primitive amplitudes (which have a fixed ordering of external legs) gauge invariant. Of course, one does not need to include the extra diagrams, but then one would need to sum over the permutations with all possible external orderings of the Higgs, as in eq. (2.5), to recover gauge invariance.

As mentioned in section 3 by observing the Feynman diagrams in fig. 4 we can write down all the scalar integrals that can enter the amplitude, see fig. 5. The integrals are two-, three- and four-point scalar integrals that have massive internal propagators and some combination of massive external kinematics. One-point tadpole integrals do not appear since they are forbidden by power counting. (When using Passarino-Veltman reduction one could encounter such integrals, but they must cancel in the final expressions for this amplitude since one does not encounter them when using Feynman parameterization.) The scalar integrals are found in appendix A.1.

In addition to the use of color decomposition, section 2.2, it is also convenient to decompose the primitive amplitudes into all possible external helicity configurations. So the objects that need to be computed are the color ordered gauge invariant primitive amplitudes. There are three such objects; they are $A_4(1^+, 2^+, 3^+, H)$, $A_4(1^+, 2^+, 3^-, H)$ and $A_4(1^+, 2^-, 3^+, H)$.

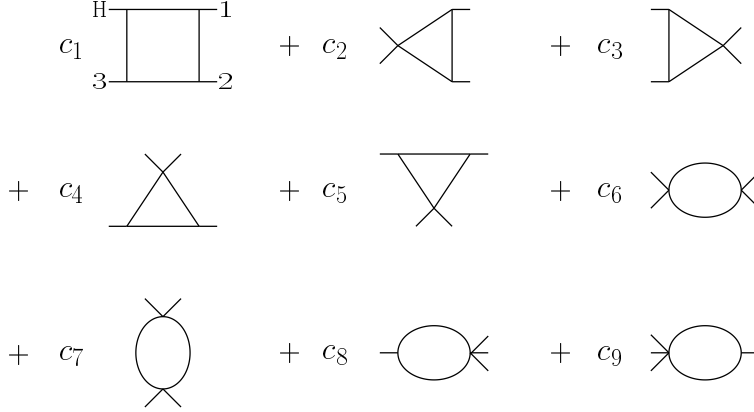


Figure 5: The $gg \rightarrow gH$ amplitude parameterized in terms of all the scalar integrals that might enter. The external legs are labeled clockwise starting at the top right.

The other primitive amplitudes (e.g. $A_4(1^-, 2^-, 3^+, H)$) can be obtained from the above three primitive amplitudes using parity and relabelings.

Since this amplitude has already been calculated by Ellis et al. [16] the purpose of the calculation is to explicitly demonstrate that we may obtain the correct results by applying the unitarity method to massive amplitudes, starting from Feynman diagrams. For illustrative purposes, only the calculation of $A_4(1^+, 2^+, 3^+, H)$ is explicitly presented here – the results of the calculation of the other two primitive amplitudes are shown for completeness.

4.1 The $A_4(1^+, 2^+, 3^+, H)$ primitive amplitude

In order to compute the primitive amplitude $A_4(1^+, 2^+, 3^+, H)$ we will construct it from multiple channels. We will see that it is sufficient to only compute the s - and t -channels. The Mandelstam variables are defined as $s \equiv (k_1 + k_2)^2$ and $t \equiv (k_2 + k_3)^2$. These channels can be seen in fig. 6.

We begin by first constructing the s -channel by sewing together the two tree amplitudes on the left- and right-hand side of fig. 6a. This corresponds to targeting the coefficients, c_1 , c_2 , c_3 and c_6 in fig. 5. The tree amplitude on the right of fig. 6a is given by [10]

$$A_4^{\text{tree}}(-L_1, 1^+, 2^+, L_2) = i \frac{[12]}{\langle 12 \rangle} \frac{\langle -L_1 | \omega_+ (\not{k} + m) | -L_2 \rangle}{(\ell_1 - k_1)^2 - \mu^2 - m^2}, \quad (4.1)$$

where $\omega_{\pm} = \frac{1}{2}(1 \pm \gamma_5)$ is the helicity projection operator and the tree amplitude on the left is given by

$$A_4^{\text{tree}}(-L_2, 3^+, H, L_1) = -\frac{im}{\sqrt{2}v} \left(\frac{\langle -L_2 | \not{k}_3^+ (\not{k}_4 - 2m) | -L_1 \rangle}{(\ell_1 + k_4)^2 - \mu^2 - m^2} + \frac{2k_4 \cdot \epsilon_3^+}{s - m_H^2} \langle -L_2 | -L_1 \rangle \right). \quad (4.2)$$

Here $v = \frac{2m_W}{g_W}$ is the vacuum expectation value of the scalar Higgs field [24], m is the mass of the fermion in the loop and m_H is the scalar Higgs mass. Capitalized momenta are $(4 - 2\epsilon)$ -dimensional, lower case momenta are four-dimensional and μ is the (-2ϵ) -dimensional part

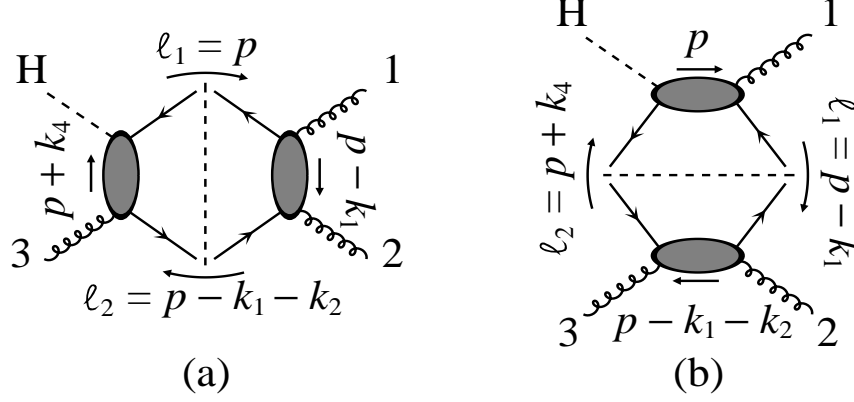


Figure 6: The s - and t -channels of the $gg \rightarrow gH$ amplitude. The on-shell lines are fermions since at tree level quarks are the only particles to couple both to gluons and to the scalar Higgs boson.

of the loop momentum. (See appendix A and appendix B.) In these tree amplitudes we follow the conventions of ref. [10] for massive spinors, summarized in appendix B. In this convention the distinction between fermion and anti-fermion spinors is suppressed.

As depicted in fig. 6a, for the s -channel the momenta of the on-shell legs are

$$\ell_1 = p, \quad \ell_2 = p - k_1 - k_2. \quad (4.3)$$

The second tree amplitude, eq. (4.2), involving the Higgs has been constructed from the tree level Feynman diagrams including the additional fictitious Higgs-Higgs-gluon coupling (this is the standard scalar-scalar-vector coupling of scalar QED [24]) mentioned earlier.

So sewing the two tree amplitudes together gives us the s -channel of the amplitude

$$A_4(1^+, 2^+, 3^+, H) \Big|_{s\text{-channel}} = - \frac{\sqrt{2}m k_4 \cdot \varepsilon_3^+}{v(s - m_H^2)} \frac{[12]}{\langle 12 \rangle} \int \frac{d^{4-2\epsilon} P}{(2\pi)^{4-2\epsilon}} \frac{\mathcal{N}_1}{\mathcal{D}_3} - \frac{m}{\sqrt{2}v} \frac{[12]}{\langle 12 \rangle} \int \frac{d^{4-2\epsilon} P}{(2\pi)^{4-2\epsilon}} \frac{\mathcal{N}_2}{\mathcal{D}_4} \Big|_{\substack{\ell_1^2 - \mu^2 - m^2 = 0 \\ \ell_2^2 - \mu^2 - m^2 = 0}}, \quad (4.4)$$

where the denominators are

$$\begin{aligned} \mathcal{D}_3 &= [\ell_1^2 - \mu^2 - m^2][(\ell_1 - k_1)^2 - \mu^2 - m^2][(\ell_1 - k_1 - k_2)^2 - \mu^2 - m^2] \\ \mathcal{D}_4 &= [\ell_1^2 - \mu^2 - m^2][(\ell_1 - k_1)^2 - \mu^2 - m^2][(\ell_1 - k_1 - k_2)^2 - \mu^2 - m^2][(\ell_1 + k_4)^2 - \mu^2 - m^2], \end{aligned} \quad (4.5)$$

and the numerators are

$$\begin{aligned} \mathcal{N}_1 &= \langle -L_1 | \omega_+(\not{p} + m) | -L_2 \rangle \langle -L_2 | -L_1 \rangle \\ \mathcal{N}_2 &= \langle -L_1 | \omega_+(\not{p} + m) | -L_2 \rangle \langle -L_2 | \not{\varepsilon}_3^+(k_4 - 2m) | -L_1 \rangle. \end{aligned} \quad (4.6)$$

The two terms in eq. (4.4) correspond to the two terms in eq. (4.2).

First, concentrating on the numerator \mathcal{N}_1 we can write it in the form of a trace

$$\mathcal{N}_1 = \text{tr}_+[(\not{\mu} + m)(\not{\ell}_2 + \not{\mu} - m)(\not{\ell}_1 + \not{\mu} - m)], \quad (4.7)$$

where we use the notation $\text{tr}_\pm[\dots] = \text{tr}[\omega_\pm \dots]$. When expanding out the trace we first concentrate on the $\not{\mu}$'s since the final expression for the numerator can only depend on μ^2 since the (-2ϵ) -dimensional integral over μ vanishes for a integrand with a odd number of μ 's. Thus,

$$\begin{aligned} \mathcal{N}_1 &= \text{tr}_+[(m\not{\ell}_2 - \mu^2 - m^2)(\not{\ell}_1 - m)] \\ &= 2m(m^2 + \mu^2) + 2m \ell_1 \cdot \ell_2 \\ &= 4m(m^2 + \mu^2) - ms. \end{aligned} \quad (4.8)$$

The numerator \mathcal{N}_2 can also be written in the form of a trace

$$\mathcal{N}_2 = \text{tr}_+[(\not{\mu} + m)(\not{\ell}_2 + \not{\mu} - m)\not{\epsilon}_3^+(\not{k}_4 - 2m)(\not{\ell}_1 + \not{\mu} - m)]. \quad (4.9)$$

So again first concentrating on the $\not{\mu}$'s we can write

$$\begin{aligned} \mathcal{N}_2 &= \text{tr}_+[(\not{\mu}\not{\ell}_2 + m\not{\ell}_2 - \mu^2 - m^2)\not{\epsilon}_3^+(\not{k}_4 - 2m)(\not{\ell}_1 + \not{\mu} - m)] \\ &= \text{tr}_+[(m\not{\ell}_2 - \mu^2 - m^2)\not{\epsilon}_3^+(\not{k}_4 - 2m)(\not{\ell}_1 - m)] - \mu^2 \text{tr}_+[\not{\ell}_2\not{\epsilon}_3^+(\not{k}_4 - 2m)] \\ &= 2m(m^2 + \mu^2)(2\ell_1 + 2\ell_2 + k_4) \cdot \varepsilon_3^+ + m \text{tr}_+[\not{\ell}_2\not{\epsilon}_3^+\not{k}_4\not{\ell}_1]. \end{aligned} \quad (4.10)$$

Recalling that $\ell_2 = \ell_1 - k_1 - k_2$ and choosing the reference momenta $q_3 = k_1$ (so that $k_1 \cdot \varepsilon_3^+ = 0$) then

$$\mathcal{N}_2 = 8m(m^2 + \mu^2)\ell_1 \cdot \varepsilon_3^+ + 6m(m^2 + \mu^2)k_4 \cdot \varepsilon_3^+ + m \text{tr}_+[\not{\ell}_2\not{\epsilon}_3^+\not{k}_4\not{\ell}_1]. \quad (4.11)$$

We can evaluate the remaining trace in the expression for \mathcal{N}_2 by using eq. (2.3)

$$\text{tr}_+[\not{\ell}_2\not{\epsilon}_3^+\not{k}_4\not{\ell}_1] = \text{tr}_-[\not{\epsilon}_3^+\not{k}_4\not{\ell}_1\not{\ell}_2] = \frac{\sqrt{2}}{\langle 13 \rangle} \langle 1^- | 4\ell_1\ell_2 | 3^- \rangle, \quad (4.12)$$

where for brevity we represent external momenta by their indices and neglect slashing the momenta inside the inner-product. Using $\not{\ell}_1\not{\ell}_2 = \not{\ell}_1(\not{\ell}_1 - \not{k}_1 - \not{k}_2) = m^2 + \mu^2 - \not{\ell}_1(\not{k}_1 + \not{k}_2)$ and momentum conservation the trace can be expressed as

$$\text{tr}_+[\not{\ell}_2\not{\epsilon}_3^+\not{k}_4\not{\ell}_1] = \frac{\sqrt{2}}{\langle 13 \rangle} \left\{ (m^2 + \mu^2) \langle 1^- | 4 | 3^- \rangle + \langle 1^- | 4\ell_1 4 | 3^- \rangle \right\}. \quad (4.13)$$

But since

$$k_4 \cdot \varepsilon_3^+ = \frac{\langle 1^- | 4 | 3^- \rangle}{\sqrt{2} \langle 13 \rangle}, \quad (4.14)$$

\mathcal{N}_2 can be expressed as

$$\mathcal{N}_2 = 8m(m^2 + \mu^2)(\ell_1 \cdot \varepsilon_3^+ + k_4 \cdot \varepsilon_3^+) + \sqrt{2}m \frac{\langle 1^- | 4\ell_1 4 | 3^- \rangle}{\langle 13 \rangle}. \quad (4.15)$$

The integral comprised of the numerator \mathcal{N}_2 now only involves at most a single power of loop momentum ℓ in the integrand. This can be readily evaluated with the use of Feynman parameterization. The Feynman parameter shift is

$$\ell_1 = q + a_2 k_1 + a_3(k_1 + k_2) - a_4 k_4, \quad (4.16)$$

where q is the shifted loop momentum. After Feynman parameterizing the integral the terms in \mathcal{N}_2 involving ℓ_1 can be evaluated by performing the momentum shift and next dropping terms containing a single power of q which vanish. So the two terms in \mathcal{N}_2 involving ℓ_1 become

$$\ell_1 \cdot \varepsilon_3^+ = \frac{\langle 1^- | q + a_2 k_1 + a_3(k_1 + k_2) - a_4 k_4 | 3^- \rangle}{\sqrt{2} \langle 13 \rangle} = -(a_3 + a_4) k_4 \cdot \varepsilon_3^+, \quad (4.17)$$

and

$$\begin{aligned} \langle 1^- | 4 \ell_1 4 | 3^- \rangle &= a_2 \langle 1^- | 414 | 3^- \rangle + a_3 \langle 1^- | 4(1+2)4 | 3^- \rangle - a_4 \langle 1^- | 444 | 3^- \rangle \\ &= [(t - m_H^2) a_2 - s a_3 - m_H^2 a_4] \langle 1^- | 4 | 3^- \rangle, \end{aligned} \quad (4.18)$$

after performing the momentum shift.

As defined in appendix A.3, the integral function $I_n[a_i]$ is a Feynman parameterized form of the loop integral with a factor of a_i in the numerator. Thus after Feynman parameterization eq. (4.4) becomes

$$\begin{aligned} A_4(1^+, 2^+, 3^+, H) \Big|_{s\text{-channel}} &= -i \frac{\sqrt{2} m^2 k_4 \cdot \varepsilon_3^+}{v(4\pi)^{2-\epsilon}} \frac{[12]}{\langle 12 \rangle} \left\{ \frac{1}{s - m_H^2} I_3^{(4)} [4(m^2 + \mu^2) - s] - (t - m_H^2) I_4[a_2] \right. \\ &\quad \left. + s I_4[a_3] + m_H^2 I_4[a_4] - 4 I_4[(m^2 + \mu^2)(1 - a_3 - a_4)] \right\} \Big|_{s\text{-channel}}, \end{aligned} \quad (4.19)$$

where $I_n^{D=4-2\epsilon}[\mu^2 a_i] = -\epsilon I_n^{D=6-2\epsilon}[a_i]$ and $I_3^{(j)}$ is defined in appendix A. The dimension label on $(4-2\epsilon)$ -dimensional integrals has been suppressed. Then using the recursive formula for $I_n[a_i]$ in eq. (A.14) and eq. (4.14) one can write the s -channel of the primitive amplitude as

$$\begin{aligned} A_4(1^+, 2^+, 3^+, H) \Big|_{s\text{-channel}} &= -\frac{i}{(4\pi)^{2-\epsilon}} \frac{m^2}{v} \frac{st}{\langle 12 \rangle \langle 23 \rangle \langle 31 \rangle} \left\{ \frac{t-u}{2t(s - m_H^2)} I_3^{(4)} [4(m^2 + \mu^2) - m_H^2] \right. \\ &\quad \left. - \frac{s - m_H^2}{2st} I_3^{(2)} [4(m^2 + \mu^2) - m_H^2] - \frac{1}{2} I_4 [4(m^2 + \mu^2) - m_H^2] \right\} \Big|_{s\text{-channel}}, \end{aligned} \quad (4.20)$$

where $u = m_H^2 - s - t$, also noting that $I_3^{(2)}$ is a scalar triangle integral dependent on the kinematic invariant s and m_H^2 , while $I_3^{(4)}$ is a function of s only. Then using eq. (A.11) the s -channel becomes

$$\begin{aligned} A_4(1^+, 2^+, 3^+, H) \Big|_{s\text{-channel}} &= -\frac{i}{(4\pi)^{2-\epsilon}} \frac{m^2}{v} \frac{st}{\langle 12 \rangle \langle 23 \rangle \langle 31 \rangle} \left\{ (4m^2 - m_H^2) \left[\frac{t-u}{2t(s - m_H^2)} I_3^{(4)} \right. \right. \\ &\quad \left. \left. - \frac{s - m_H^2}{2st} I_3^{(2)} - \frac{1}{2} I_4 \right] - 4\epsilon \left[\frac{t-u}{2t(s - m_H^2)} I_3^{(4)D=6-2\epsilon} - \frac{s - m_H^2}{2st} I_3^{(2)D=6-2\epsilon} - \frac{1}{2} I_4^{D=6-2\epsilon} \right] \right\} \Big|_{s\text{-channel}}. \end{aligned} \quad (4.21)$$

Now that we have the s -channel of this amplitude we need to calculate the t -channel (corresponding to targeting c_1, c_4, c_5 and c_7 in fig. 5) in order to reconstruct the full primitive amplitude. However due to the symmetry of the all-plus primitive amplitude it is not necessary to explicitly perform this calculation as the s - and t -channels are related up to an overall sign by a simple exchange of legs 1 and 3 which is equivalent to exchanging s and t in eq. (4.21) (and also switching the 1 and 3 in the inner products in the pre-factor of the expression). Thus the t -channel of $A_4(1^+, 2^+, 3^+, H)$ is given by

$$A_4(1^+, 2^+, 3^+, H) \Big|_{t\text{-channel}} = -\frac{i}{(4\pi)^{2-\epsilon}} \frac{m^2}{v} \frac{st}{\langle 12 \rangle \langle 23 \rangle \langle 31 \rangle} \left\{ (4m^2 - m_H^2) \left[\frac{s-u}{2s(t-m_H^2)} I_3^{(1)} \right. \right. \\ \left. \left. - \frac{t-m_H^2}{2st} I_3^{(3)} - \frac{1}{2} I_4 \right] - 4\epsilon \left[\frac{s-u}{2s(t-m_H^2)} I_3^{(1)D=6-2\epsilon} - \frac{t-m_H^2}{2st} I_3^{(3)D=6-2\epsilon} - \frac{1}{2} I_4^{D=6-2\epsilon} \right] \right\} \Big|_{t\text{-channel}}, \quad (4.22)$$

again recalling that $I_3^{(3)}$ is a scalar triangle integral dependent on the kinematic invariant t and m_H^2 , while $I_3^{(1)}$ is a function of t only. It is also useful to observe that the coefficient of the I_4 integral in the t -channel matches that of the s -channel as expected. If we refer back to fig. 5, where all the scalar integrals that could possibly enter were listed, we notice that the coefficients, c_8 of $I_2(m_H^2)$ and c_9 of $I_2(0)$ have not yet been fixed. However, there are no other UV infinities in either the s - or t -channel expressions (eqs. (4.21) and (4.22)), so therefore since this primitive amplitude is UV-finite (since it vanishes at tree level), it is not surprising that these coefficients are zero. This may be explicitly verified by direct construction of the channel corresponding to using the on-shell condition on the two propagators adjacent to the massive external leg, showing that both c_8 and c_9 are individually zero. We have not evaluated this channel, since this example is only for illustrative purposes.

Thus with the two channels of the primitive amplitude we can construct the full primitive amplitude $A_4(1^+, 2^+, 3^+, H)$, which is

$$A_4(1^+, 2^+, 3^+, H) = -\frac{i}{(4\pi)^{2-\epsilon}} \frac{m^2}{v} \frac{st}{\langle 12 \rangle \langle 23 \rangle \langle 31 \rangle} \left\{ (4m^2 - m_H^2) \left[\frac{s-u}{2s(t-m_H^2)} I_3^{(1)} - \frac{s-m_H^2}{2st} I_3^{(2)} \right. \right. \\ \left. \left. - \frac{t-m_H^2}{2st} I_3^{(3)} + \frac{t-u}{2t(s-m_H^2)} I_3^{(4)} - \frac{1}{2} I_4 \right] - 4\epsilon \left[\frac{s-u}{2s(t-m_H^2)} I_3^{(1)D=6-2\epsilon} \right. \right. \\ \left. \left. - \frac{s-m_H^2}{2st} I_3^{(2)D=6-2\epsilon} - \frac{t-m_H^2}{2st} I_3^{(3)D=6-2\epsilon} + \frac{t-u}{2t(s-m_H^2)} I_3^{(4)D=6-2\epsilon} - \frac{1}{2} I_4^{D=6-2\epsilon} \right] \right\}. \quad (4.23)$$

Note that this expression is valid to all orders in ϵ with four-dimensional external momenta. Since this amplitude has no ultraviolet or quadratic divergences, the primitive amplitude is well defined in the limit $\epsilon \rightarrow 0$. Therefore eq. (4.23) can be simplified, since in this limit with the use of eq. (A.8), $\epsilon I_3^{D=6-2\epsilon} \rightarrow \frac{1}{2}$ and $\epsilon I_4^{D=6-2\epsilon} \rightarrow 0$. Also with the intention of simplifying

this expression we can use eq. (A.5) explicitly. Thus

$$\begin{aligned}
A_4(1^+, 2^+, 3^+, H) = & -\frac{i}{(4\pi)^2} \frac{m^2}{v} \frac{st}{\langle 12 \rangle \langle 23 \rangle \langle 31 \rangle} \left\{ (4m^2 - m_H^2) \left[\frac{1}{s - m_H^2} I_3(s) + \frac{1}{t - m_H^2} I_3(t) \right] \right. \\
& \left. + \frac{m_H^2}{st} I_3(m_H^2) - \frac{1}{2} I_4(s, t, m_H^2) \right] - \frac{2u(m_H^4 - ts)}{ts(s - m_H^2)(t - m_H^2)} \left. \right\},
\end{aligned} \tag{4.24}$$

where all the integrals in this equation are in four dimensions.

4.2 The remaining primitive amplitudes

In a similar fashion to the all-plus helicity case the primitive amplitudes corresponding to the remaining two helicity configurations may be calculated. The results are

$$\begin{aligned}
A_4(1^+, 2^+, 3^-, H) = & -\frac{i}{(4\pi)^2} \frac{m^2}{v} \frac{[12]^3}{[13][23]} \frac{t}{s} \left\{ \frac{4um^2}{(t - m_H^2)^2} I_3(t) - \frac{4um^2 m_H^2}{t(t - m_H^2)^2} I_3(m_H^2) \right. \\
& + (4m^2 - s) \left[\frac{1}{s - m_H^2} I_3(s) + \frac{1}{t - m_H^2} I_3(t) - \frac{m_H^2}{t(t - m_H^2)} I_3(m_H^2) - \frac{1}{2} I_4(s, t, m_H^2) \right] \\
& \left. - \frac{2u}{(t - m_H^2)^2} [\tilde{I}_2(t) - \tilde{I}_2(m_H^2)] + \frac{2u(t - s)}{t(s - m_H^2)(t - m_H^2)} \right\},
\end{aligned} \tag{4.25}$$

and

$$\begin{aligned}
A_4(1^+, 2^-, 3^+, H) = & -\frac{i}{(4\pi)^2} \frac{m^2}{v} \frac{[13]^3}{[12][23]} \frac{st}{u^2} \left\{ -\frac{1}{2} \left[u - 12m^2 - \frac{4ts}{u} \right] I_4(s, t, m_H^2) \right. \\
& + \left[\frac{u - 4m^2}{s - m_H^2} + \frac{4s}{u} + \frac{4um^2}{(s - m_H^2)^2} \right] I_3(s) + \left[\frac{u - 4m^2}{t - m_H^2} + \frac{4t}{u} + \frac{4um^2}{(t - m_H^2)^2} \right] I_3(t) \\
& + m_H^2 \left[\frac{(u - 4m^2)(st - u^2)}{st(s - m_H^2)(t - m_H^2)} - \frac{4}{u} - \frac{4um^2}{s(s - m_H^2)^2} - \frac{4um^2}{t(t - m_H^2)^2} \right] I_3(m_H^2) \\
& \left. - \frac{2(3u + 2t)}{(s - m_H^2)^2} [\tilde{I}_2(s) - \tilde{I}_2(m_H^2)] - \frac{2(3u + 2s)}{(t - m_H^2)^2} [\tilde{I}_2(t) - \tilde{I}_2(m_H^2)] - \frac{2u(u^2 - st)}{st(s - m_H^2)(t - m_H^2)} \right\},
\end{aligned} \tag{4.26}$$

where the \tilde{I}_2 's are bubble integrals with their $1/\epsilon$ poles removed (since the poles cancel in the difference between the two I_2 's) and all integrals are in four dimensions.

Thus in equations (4.24,4.25,4.26) we have the three necessary primitive amplitudes $A_4(1^+, 2^+, 3^+, H)$, $A_4(1^+, 2^+, 3^-, H)$ and $A_4(1^+, 2^-, 3^+, H)$ which are needed for the full $gg \rightarrow gH$ amplitude. We have compared these amplitudes to those of Ellis et al. [16] and they agree. This comparison is performed by dotting the tensor expressions of Ellis et al. with spinor helicity polarization vectors.

5 Summary and discussion

In this paper we have explained the relationship of the unitarity method reviewed in ref.[1] to Feynman diagram calculations. One may calculate Feynman diagrams in a sophisticated manner so as to take advantage of the benefits of the unitarity method. We have illustrated the usefulness of this method for the case of $gg \rightarrow gH$. This example is general in that it incorporates both massive internal and external kinematics as well as a combination of colored and colorless external particles. It should be evident from the explicit calculation presented in this paper that this method lends itself to making complicated analytical calculations more tractable. This is because in this approach one is always dealing with gauge invariant constructions, which are generally significantly simpler than the gauge dependent Feynman graphs in a conventional calculation. In the unitarity method one targets the coefficients of a subset of scalar integrals contributing to the amplitude by computing a gauge invariant combination of Feynman diagrams.

The notion of a channel as defined in this paper is more general than just the cut legs of a Cutkosky calculation, where one is nominally computing the discontinuity of an amplitude in a certain cut channel. The reason it is more general is that one defines a channel as a subset of the terms in the full amplitude; those terms being the scalar integrals that include some pre-defined combination of internal propagators. This notion of a channel has already been useful in the evaluation of $Z \rightarrow 4$ partons [13]. It was also helpful in two-loop calculations in $N = 4$ supersymmetric Yang-Mills [15].

One of the themes of this paper has been to explain the usefulness of the unitarity method to multi-point one-loop calculations. The ideas discussed here will potentially be beneficial to the extension of these types of calculations to multi-loops. Initial steps have already been made [15], and more attention is being devoted to these pursuits.

Acknowledgments

I thank Z. Bern for encouragement and many valuable discussions. I also thank L. Dixon, A.K. Grant, D.A. Kosower, E. Marcus, A.G. Morgan and B. Yan for helpful discussions and comments. This work was supported by the DOE under contract DE-FG03-91ER40662.

A Integrals

In this appendix we collect expressions for the integrals [21, 25, 26] we use in this paper. The D -dimensional loop integrals considered in this paper are defined by

$$I_n^D[P^{\alpha_1} \dots P^{\alpha_m}] = i(-1)^{n+1}(4\pi)^{D/2} \int \frac{d^D P}{(2\pi)^D} \frac{P^{\alpha_1} \dots P^{\alpha_m}}{(P^2 - m^2) \dots ((P - \sum_{i=1}^{n-1} k_i)^2 - m^2)}, \quad (\text{A.1})$$

where P is a D -dimensional momentum and the external momenta, k_i , are four-dimensional. Our convention is to suppress the dimension label on I_n when we are dealing with a $D = 4 - 2\epsilon$ integral, unless otherwise indicated. We also suppress the square brackets when the argument is unity. Such integrals are referred to in the text as scalar integrals, while tensor integrals have $m \geq 1$.

Given a four-point amplitude, we have two conventions for labeling the one-, two- and three-point integrals. The first, and more familiar one is to explicitly give the kinematic invariant upon which the integral depends. For example, $I_2(s)$ is the $(4 - 2\epsilon)$ -dimensional bubble that has an invariant mass square of $s = (k_1 + k_2)^2$ flowing through its external legs. The second convention for labeling the lower point integrals is to indicate, by a raised (i) that the internal propagator between legs $i - 1 \pmod{4}$ and i has been removed. If two indices are present as in (i, j) then two propagators have been removed. This follows the labeling convention of refs. [26, 10].

A.1 The $D = 4 - 2\epsilon$ scalar integrals

The bubble with an external kinematic invariant s is

$$I_2(s) = I_2^{(2,4)} = I_2(0) + 2 + x \log\left(\frac{x-1}{x+1}\right) + \mathcal{O}(\epsilon), \quad (\text{A.2})$$

where $x \equiv \sqrt{1 - 4m^2/s}$. For external massless kinematics, this may be written in closed form as

$$I_2(0) = m^{-2\epsilon} \frac{\Gamma(1 + \epsilon)}{\epsilon}. \quad (\text{A.3})$$

The scalar triangle integral can either be a function of just one kinematic invariant s

$$I_3(s) = I_3^{(4)} = -\frac{1}{2s} \log^2\left(\frac{x+1}{x-1}\right) + \mathcal{O}(\epsilon), \quad (\text{A.4})$$

or of two invariants s and m_H^2

$$I_3(s, m_H^2) = I_3^{(2)} = \frac{sI_3(s) - m_H^2 I_3(m_H^2)}{s - m_H^2} + \mathcal{O}(\epsilon). \quad (\text{A.5})$$

While the box with a uniform internal mass and a single massive external leg, with invariant mass-square m_H^2 is

$$I_4(s, t, m_H^2) = -\frac{1}{st} \left[H\left(-\frac{um^2}{st}, \frac{m^2}{s}\right) + H\left(-\frac{um^2}{st}, \frac{m^2}{t}\right) - H\left(-\frac{um^2}{st}, \frac{m^2}{m_H^2}\right) \right] + \mathcal{O}(\epsilon), \quad (\text{A.6})$$

where $u = m_H^2 - s - t$,

$$H(X, Y) \equiv \frac{2}{x_+ - x_-} \left[\ln\left(1 - \frac{X}{Y}\right) \ln\left(\frac{-x_-}{x_+}\right) - \text{Li}_2\left(\frac{x_-}{y - x_+}\right) - \text{Li}_2\left(\frac{x_-}{x_- - y}\right) + \text{Li}_2\left(\frac{x_+}{x_+ - y}\right) + \text{Li}_2\left(\frac{x_+}{y - x_-}\right) \right], \quad (\text{A.7})$$

with $x_{\pm} = \frac{1}{2}(1 \pm \sqrt{1 - 4X})$, $y = \frac{1}{2}(1 + \sqrt{1 - 4Y})$ and the dilogarithm [27] is defined by $\text{Li}_2(x) \equiv -\int_0^1 dt \ln(1 - xt)/t$.

The scalar integral expressions quoted above are only valid in certain analytic regions. These can be analytically continued, but are not presented here since related expressions² are presented for all analytic regions in ref. [16].

²The relationship between the scalar integrals in this paper and those in ref. [16]: $I_2(s) = I_2(0) + 2 - W_1(s)$, $I_3(s) = -W_2(s)/2s$ and $I_4(s, t, m_H^2) = -W_3(s, u, t, m_H^2)/st$.

A.2 Higher dimension integrals

The higher dimension integrals are defined in eq. (A.1) with D set to the appropriate value. The relationship of these integrals to the usual four-dimensional ones has been extensively discussed in ref. [26]. For $n \leq 6$, $(6 - 2\epsilon)$ -dimensional integrals can be written in terms of $(4 - 2\epsilon)$ -dimensional integrals via the integral recursion relation

$$I_n^{D=6-2\epsilon} = \frac{1}{(n-5+2\epsilon)c_0} \left[2I_n^{D=4-2\epsilon} - \sum_{i=1}^n c_i I_{n-1}^{(i), D=4-2\epsilon} \right], \quad (\text{A.8})$$

where $c_i = \sum_{j=1}^4 S_{ij}^{-1}$, $c_0 = \sum_{i=1}^n c_i$, and the matrix S_{ij} is

$$S_{ij} \equiv m^2 - \frac{1}{2} p_{ij}^2, \quad \text{with } p_{ii} \equiv 0, \quad \text{and } p_{ij} = p_{ji} \equiv k_i + k_{i+1} + \dots + k_{j-1} \quad \text{for } i < j. \quad (\text{A.9})$$

Higher dimension integrals arise naturally when performing the calculations described in this paper. In a typical primitive amplitude discussed in the text we obtain integrals of the form

$$I_n^{D=4-2\epsilon}[f(p^\alpha, k_i^\alpha, \mu^2)] = i(-1)^{n+1} (4\pi)^{2-\epsilon} \int \frac{d^4 p}{(2\pi)^4} \frac{d^{-2\epsilon} \mu}{(2\pi)^{-2\epsilon}} \frac{f(p^\alpha, k_i^\alpha, \mu^2)}{(p^2 - \mu^2 - m^2) \dots ((p - \sum_{i=1}^{n-1} k_i)^2 - \mu^2 - m^2)}, \quad (\text{A.10})$$

where we have explicitly broken the $(4 - 2\epsilon)$ -dimensional momentum into a four-dimensional part, p , and a (-2ϵ) -dimensional part, μ .

As noted by Mahlon [6], using the definition (A.1), we can write

$$I_n^{D=4-2\epsilon}[\mu^2] = -\epsilon I_n^{D=6-2\epsilon}. \quad (\text{A.11})$$

Note that although the loop momentum is shifted to higher dimension, the external momenta remain in four dimensions.

A.3 Feynman parameter reduction

As discussed in the text, tensor integrals may be evaluated using Feynman parameters. We make use of the following formulae in the text.

After Feynman parameterization and the normal shift of momentum we make use of the following,

$$\int \frac{d^4 q}{(2\pi)^4} \frac{d^{-2\epsilon} \mu}{(2\pi)^{-2\epsilon}} \frac{q^{\alpha_1} \dots q^{\alpha_{2r+1}}}{(q^2 - \mu^2 - S_{ij} a_i a_j)^n} = 0, \quad (\text{A.12})$$

where S_{ij} is defined in eq. (A.9).

After integrating out the loop momenta we obtain integrals of the form

$$I_n^D[f(a_k)] \equiv \Gamma(n - D/2) \int_0^1 d^n a_k \delta(1 - \sum_r a_r) \frac{f(a_k)}{\left[\sum_{i,j=1}^n S_{ij} a_i a_j - i\epsilon \right]^{n-D/2}}. \quad (\text{A.13})$$

An integral reduction formula that is quite useful is [26]

$$I_n^D[a_i] = \frac{1}{2} \sum_{j=1}^n c_{ij} I_{n-1}^{(j),D} + \frac{c_i}{c_0} I_n^D, \quad (\text{A.14})$$

where $c_{ij} = S_{ij}^{-1} - \frac{c_i c_j}{c_0}$, and c_i and c_0 are defined in appendix A.2. Another useful integral reduction formula for $I_n^D[a_i a_j]$ can also be found in [26].

B Rules for μ 's

To begin, we have a $(4 - 2\epsilon)$ -dimensional vector, Q^α , which we can express as a sum of a four dimensional piece q^α and a (-2ϵ) -dimensional μ^α ; $Q^\alpha = q^\alpha + \mu^\alpha$. (We have used the convention that upper-case momenta are $(4 - 2\epsilon)$ -dimensional and lower-case momenta are four-dimensional.) Here we summarize the rules for dealing with μ 's given in ref. [10].

We abide by the conventional Dirac algebra, $\{\gamma^\alpha, \gamma^\beta\} = 2\eta^{\alpha\beta}$ and $\gamma^{\alpha\dagger}\gamma^0 = \gamma^0\gamma^\alpha$, where α and β are $(4 - 2\epsilon)$ -dimensional Lorentz indices. The metric is given by $\eta^{\alpha\beta} = \text{diag}(+, -, -, -, \dots)$. It follows that $Q \cdot Q = q^2 - \mu^2$ (the negative sign preceding the μ^2 is from the metric).

Thus $\not{\mu}$ anti-commutes with four-dimensional γ^α matrices, $\{\not{q}, \not{\mu}\} = 0$. So if we use the conventions of 't Hooft and Veltman [28], and adopt the arbitrary dimension definition, $\gamma_5 = i\gamma^0\gamma^1\gamma^2\gamma^3$, then $\{\not{q}, \gamma_5\} = 0$ and $[\not{\mu}, \gamma_5] = 0$. That is $\not{\mu}$ freely commutes with γ_5 , since γ_5 is constructed as a product of four-dimensional Dirac matrices. Hence, $\omega_\pm \not{q} = \not{q} \omega_\mp$ and $\omega_\pm \not{\mu} = \not{\mu} \omega_\pm$, where $\omega_\pm \equiv \frac{1}{2}(1 \pm \gamma_5)$ is the helicity projection operator. In calculations it is important to first commute the $\not{\mu}$'s together before evaluating the remaining four-dimensional pieces.

In the calculation presented in section 4 the momentum of the sewn fermion lines is $(4 - 2\epsilon)$ -dimensional. We will borrow the bra and ket symbols to represent the spinors, but as helicity is not a good quantum number we shall not label them with a helicity. Since we always sum over all states across the cut, there is no need to define a $(4 - 2\epsilon)$ helicity notion.

In sewing the $(4 - 2\epsilon)$ -spinors together we implicitly sum over the spin degrees of freedom, that is

$$|Q\rangle\langle Q| = \not{Q} + m = \not{q} + \not{\mu} + m, \quad \text{and} \quad |-Q\rangle\langle -Q| = -\not{Q} + m = -\not{q} - \not{\mu} + m. \quad (\text{B.1})$$

This notation glosses over the distinction of spinors and anti-spinors. However, as discussed in ref. [10], this may introduce an overall sign which can be readily fixed by hand. Alternatively, one may easily use both particle and anti-particle spinors to obtain identical results.

References

- [1] Z. Bern, L. Dixon and D.A. Kosower, Ann. Rev. Nucl. Part. Sci. 46:109 (1996), hep-ph/9602280.

- [2] F.A. Berends, R. Kleiss, P. De Causmaecker, R. Gastmans and T. T. Wu, Phys. Lett. B103:124 (1981);
P. De Causmaecker, R. Gastmans, W. Troost and T.T. Wu, Nucl. Phys. B206:53 (1982);
R. Kleiss and W.J. Stirling, Nucl. Phys. B262:235 (1985);
Z. Xu, D.-H. Zhang and L. Chang, Nucl. Phys. B291:392 (1987).
- [3] J.E. Paton and Chan Hong-Mo, Nucl. Phys. B10:519 (1969);
F.A. Berends and W.T. Giele, Nucl. Phys. B294:700 (1987);
D.A. Kosower, B.-H. Lee and V.P. Nair, Phys. Lett. 201B:85 (1988);
M. Mangano, S. Parke and Z. Xu, Nucl. Phys. B298:653 (1988);
Z. Bern and D.A. Kosower, Nucl. Phys. B362:389 (1991).
- [4] Z. Bern and D.A. Kosower, Nucl. Phys. B379:451 (1992).
- [5] F.A. Berends and W.T. Giele, Nucl. Phys. B306:759 (1988);
D.A. Kosower, Nucl. Phys. B335:23 (1990);
G. Mahlon and T.-M. Yan, Phys. Rev. D47:1776 (1993), hep-ph/9210213;
G. Mahlon, Phys. Rev. D47:1812 (1993), hep-ph/9210214;
G. Mahlon, T.-M. Yan and C. Dunn, Phys. Rev. D48:1337 (1993), hep-ph/9210212;
C. Kim and V.P. Nair, Phys. Rev. D55:3851 (1997), hep-th/9608156.
- [6] G. Mahlon, Phys. Rev. D49:2197 (1994), hep-ph/9311213; Phys. Rev. D49:4438 (1994), hep-ph/9312276.
- [7] L.D. Landau, Nucl. Phys. 13:181 (1959);
S. Mandelstam, Phys. Rev. 112:1344 (1958), 115:1741 (1959);
R.E. Cutkosky, J. Math. Phys. 1:429 (1960).
- [8] Z. Bern, L. Dixon, D.C. Dunbar and D.A. Kosower, Nucl. Phys. B425:217 (1994), hep-ph/9403226.
- [9] Z. Bern, L. Dixon, D.C. Dunbar and D.A. Kosower, Nucl. Phys. B435:59 (1995), hep-ph/9409265.
- [10] Z. Bern and A.G. Morgan, Nucl. Phys. B467:479 (1996), hep-ph/9511336.
- [11] S.J. Parke and T.R. Taylor, Phys. Rev. Lett. 56:2459 (1986);
Z. Bern, L. Dixon and D.A. Kosower, *Proceedings of Strings 1993*, eds. M.B. Halpern, A. Sevrin and G. Rivlis (World Scientific, Singapore, 1994), hep-th/9311026;
Z. Bern, G. Chalmers, L. Dixon and D.A. Kosower, Phys. Rev. Lett. 72:2134 (1994), hep-ph/9312333;
Z. Bern and G. Chalmers, Nucl. Phys. B447:465 (1995), hep-ph/9503236.
- [12] Z. Bern, L. Dixon and D.A. Kosower, Phys. Rev. Lett. 70:2677 (1993), hep-ph/9302280;
Z. Kunszt, A. Signer and Z. Trócsányi, Phys. Lett. B336:529 (1994), hep-ph/9405386;
Z. Bern, L. Dixon and D.A. Kosower, Nucl. Phys. B437:259 (1995), hep-ph/9409393.

- [13] Z. Bern, L. Dixon and D.A. Kosower, Nucl. Phys. Proc. Suppl. 51C:243 (1996), hep-ph/9606378;
Z. Bern, L. Dixon, D.A. Kosower and S. Weinzierl, Nucl. Phys. B489:3 (1997), hep-ph/9610370;
Z. Bern, L. Dixon and D.A. Kosower, preprint hep-ph/9708239.
- [14] W.L. van Neerven, Nucl. Phys. B268:453 (1986).
- [15] Z. Bern, J.S. Rozowsky and B. Yan, Phys. Lett. B401:273 (1997), hep-ph/9702424.
- [16] R.K. Ellis, I. Hinchliffe, M. Soldate and J.J. Van Der Bij, Nucl. Phys. B297:221 (1988).
- [17] M. Mangano and S.J. Parke, Phys. Rep. 200:301 (1991);
L. Dixon, *Proceedings of Theoretical Advanced Study Institute in Elementary Particle Physics (TASI 95)*, ed. D.E. Soper, hep-ph/9601359.
- [18] W. Siegel, Phys. Lett. B84:193 (1979);
D.M. Capper, D.R.T. Jones and P. van Nieuwenhuizen, Nucl. Phys. B167:479 (1980);
S.J. Gates, M.T. Grisaru, M. Rocek and W. Siegel, *Superspace*, (Benjamin/Cummings, 1983).
- [19] Z. Kunszt, A. Signer and Z. Trócsányi, Nucl. Phys. B411:397 (1994), hep-ph/9305239;
S. Catani, M.H. Seymour and Z. Trócsányi, Phys. Rev. D55:6819 (1997), hep-ph/9610553.
- [20] Z. Bern, L. Dixon and D.A. Kosower, Nucl. Phys. B437:259 (1995), hep-ph/9409393.
- [21] L.M. Brown and R.P. Feynman, Phys. Rev. 85:231 (1952);
L.M. Brown, Nuovo Cimento 21:3878 (1961);
G. Passarino and M. Veltman, Nucl. Phys. B160:151 (1979).
- [22] R. Pittau, preprint hep-ph/9607309.
- [23] G. 't Hooft, in *Acta Universitatis Wratislavenensis no. 38, 12th Winter School of Theoretical Physics in Karpacz; Functional and Probabilistic Methods in Quantum Field Theory*, Vol. 1 (1975);
B.S. DeWitt, in *Quantum gravity II*, eds. C. Isham, R. Penrose and D. Sciama (Oxford, 1981);
L.F. Abbott, Nucl. Phys. B185:189 (1981).
- [24] M. Peskin and D.V. Schroeder, *An Introduction to Quantum Field Theory* (Addison-Wesley, 1995).
- [25] G. 't Hooft and M. Veltman, Nucl. Phys. B153:365 (1979);
A. Denner, U. Nierste and R. Scharf, Nucl. Phys. B367:637 (1991);
W. van Neerven and J.A.M. Vermaseren, Phys. Lett. B137:241 (1984);
G.J. van Oldenborgh and J.A.M. Vermaseren, Zeit. Phys. C46:425 (1990).

- [26] Z. Bern, L. Dixon and D.A. Kosower, Phys. Lett. B302:299 (1993), hep-ph/9212308; erratum *ibid.* B318:649 (1993);
Z. Bern, L. Dixon and D.A. Kosower, Nucl. Phys. B412:751 (1994), hep-ph/9306240.
- [27] L. Lewin, *Polylogarithms and Associated Functions* (North Holland, 1981).
- [28] G. 't Hooft and M. Veltman, Nucl. Phys. B44:189 (1972).